Received: 28 July 2021 | Revised: 17 September 2021 | Accepted: 17 September 2021

DOI: 10.1002/er.7329

RESEARCH ARTICLE

INTERNATIONAL JOURNAL OF ENERGY RESEARCH WILEY

# Sandwich assembly of sulfonated poly (ether sulfone) with sulfonated multiwalled carbon nanotubes as an efficient architecture for enhanced electrolyte performance in $H_2/O_2$ fuel cells

**Gayathri Ravi Kumar**[1] | **Cao Guozhong**[2] | **Ramesh Prabhu Manimuthu**[1]

[1]Department of Physics, Alagappa University, Karaikudi, India

[2]Department of Materials Science and Engineering, University of Washington, Seattle, Washington, USA

**Correspondence**
Ramesh Prabhu Manimuthu, Department of Physics, Alagappa University, Karaikudi, 630 003, Tamil Nadu, India.
Email: rameshprabhum@alagappauniversity.ac.in

**Summary**

Proton exchange membrane (PEM) for $H_2/O_2$ fuel cell are made as sandwich assembly of sulfonated poly(ether sulfone) (SPES) with sulfonic acid functionalized multiwalled carbon nanotubes (SMWCNT). The SMWCNT occupies at the middle layer enhances the interfacial interplay and interconnects the nano-phase separation via hydrogen bond between the sulfonic acid of SPES and SMWCNT. The sandwich structure improves the integration of hydrophilic and hydrophobic layers of SPES and SMWCNT, that obliviously enhance the tensile and mechanical property of the membrane. Thus promotes the continuous proton conducting channels through the sandwiched morphology by using the proton hopping mechanism. The 1.5 wt% of SMWCNT in SPES (G3) offers high proton conductivity, current and power density values at 80°C under 100% RH, which are $72.0 \times 10^{-3}$ S cm$^{-1}$, 778.26 mA cm$^{-2}$ and 173.29 mW cm$^{-2}$, respectively. Within addition to remarkable durability, the OCV degradation is about 0.02 V after 15 hours of durability test and $H_2$ permeability of 2.14 barrer. The excellent thermal stability of 91.2 wt% at 150°C and the Young's modulus of 2208 ± 110 MPa was attained by the G3, which strongly suggest that the promising nature of PEM.

**KEYWORDS**

electrochemical performance, multiwalled carbon nanotubes, proton exchange membranes, sandwich membranes, sulfonated poly (ether sulfone)

## 1 | INTRODUCTION

Materials and technologies for sustainable clean energy are a matter of great concern in the present era, owing to the depletion of non-renewable energy resources and increasing awareness of the environment and health. The fuel cells that transform the chemical energy into electricity are considered as the effectual power output, higher conversion efficiency, long shelf/cycle life and environmental friendly. The proton exchange membrane fuel cell (PEMFC) is considered as the good power generation system for its unique characteristics such as quick start up with high efficiency and energy density at low resource consumption and environmental impact. In PEMFC, the polymer electrolyte membrane (PEM) plays a crucial role in determining power conversion efficiency.[1-4] The ideal PEM should possess high ionic conduction and low electronic conductivity with excellent thermal, chemical and mechanical stability. The fluorinated carbon membrane Nafion, developed by DuPont, is

  

widely used as PEM for PEMFC. However, there are several drawbacks of using Nafion at high temperatures that hinder their practical applications. Nafion membranes possess dehydration property at temperatures above 80°C and low humidity, which causes decrease in the proton conductivity and mechanical stability. Its restricted perfluorosulfonic acid structure with fluorine containing groups and higher cost hinders its commercialization as PEM.[5-9]

Recent progress in PEM material has demonstrated the sulfonated poly(ether sulfone) (SPES) polymer as the best substitute for the traditional benchmark membrane of Nafion compared to other sulfonated polymers.[10-16] SPES exhibits a better performance compared to sulfonated poly(aryl sulfone)s and sulfonated poly(aryl ether sulfone)s with the same sulfone backbones. The sulfonated poly(aryl sulfone)s offers a flexible membrane due to its rigid aromatic structure, but this structure preserves the water molecules and causes the excessive swelling in the membrane, which allows the low resistance fuel crossover and finally deploy the polarization performance. Also the sulfonated poly(aryl ether sulfone)s with its brittleness nature and excessive swelling can only be used as PEM when it is polar substituted on its backbone or cross linked with other polymers.[17-19] The electrophilic aromatic sulfonation of PES creates negatively charged sulfonic acid groups on the PES matrix that improves its hydrophilicity. The SPES allows for the hydrophobic and hydrophilic character that credits excellent mechanical, thermal stability and enhanced proton conductivity. The SPES is chosen for its superb film-forming ability, easily functionalized and available as a commercial membrane with a low cost.[20-24] An issue with the pure SPES membrane is that it still has less connected ionic channels that affect the proton conductivity for the constructive PEMFC operation. The efforts overcame the technical bottleneck of SPES by grafting with the metal-organic framework, sulfonated graphene oxide (SGO), phosphotungstic acid (PWA), cellulose nanofibers, sulfonated molybdenum disulfide (S-$MoS_2$) and chitin nanowhisker.[24-29] Infusion of such nano-fillers changes the interfacial interaction of the membrane. Thus, the stability, proton conductivity and fuel crossover resistance of the nanocomposite membrane at elevated temperatures will be improved. The framework of an organic polymer matrix with inorganic nano-fillers makes a practical strategy to fabricate unique PEM.

Carbon-based inorganic nano-filler with exceptional properties have attracted increasing attention for a wide range of applications, though predominantly in the clean and sustainable energy sector. Multiwalled carbon nanotubes (MWCNT) are a fascinating material with a high specific surface area, excellent electrochemical stability and mechanical property. The multiwalled carbon nanotubes comprise concentrical multiple nested graphene sheets with an interlayer distance similar to that in graphite.[30] The pure MWCNT is hydrophobic and not dispersed in water, paid for its high surface area and strong Van Der Waals forces that urge for functionalization.[31] Before adding within the polymer matrix, the sulfonic acid groups functionalization onto the walls of MWCNT (SMWCNT) was done to enrich the chemical stability. It de-bundle the MWCNT aggregate consequences in homogenous dispersion and hydrophilicity of the membrane than the MWCNT. Moreover, higher surfactant concentration can reduce the nanocomposites electrical properties since it forms an insulating layer around the tubes.[32] Yin et al[33] also achieved the proton conductivity of 0.03 S $cm^{-1}$ for SMWCNT with Nafion, which is higher than the proton conductivity of MWCNT-Nafion (0.01 S $cm^{-1}$).

Although the SMWCNT has demonstrated incredible guaranteed nano-filler in improving the quality of electrolyte films, there stays a possibility of aggregation and disordered distribution in the nanocomposite films mainly made with solvent casting technique. Even the layer-by-layer (LBL) technique is widely used friendly method to prepare the multilayer electrolyte membranes with its easy preparation and low cost. Inappropriately, the electrolyte membrane organized via the LBL technique finds hardship in hydroxyl conduction and acts as a significant barrier in the cell performance of PEMFC. And its extreme membrane synthesis process also raises the membrane cost.[34] To reach the synergistic membrane property, the grafting of SMWCNT onto the SPES matrix as a sandwich membrane act as a proper membrane modification strategy. The electrolyte membrane made as sandwich structure possesses good hydrolytic and thermal stability and ultimately resists the fuel crossover in PEMFC performance. Besides the electrostatic attraction, the SPES/SMWCNT/SPES possess a strong hydrogen bonding from the super sulfonic acid group, which would ultimately form a compatible layer-by-layer sandwich nanocomposite membrane. Researchers also reported the similar findings of the sandwich nanocomposite membranes for various polymers with other nano-fillers. Kannan et al[35] constructed a three-layered membrane of phosphoric acid doped PBI that showed lower voltage decay than a single-layered membrane. Jia et al[36] formed the phosphoric acid doped and undoped $(PU/GO/PDDA/GO)_{200}$ layered membrane. They found the phosphoric acid doped $(PU/GO/PDDA/GO)_{200}$/60%PA membrane is a highly stable proton conduction membrane with good mechanical stability. Che et al[37] synthesized the multicomponent membrane of $(SPEEK/PU/SPEEK/bmim)_{100}$/60%PA. It reached the maximum proton

conduction with the mechanical stability than the undoped of the phosphoric acid multicomponent membrane. Li et al[38] prepared the SPEEK/SGO/SPEEK sandwich membrane to increase the proton conductivity than the SPEEK/GO/SPEEK sandwich membrane. The construction of PEM with SPES/SMWCNT/SPES was employed here for the first time.

This research's primary intention is to develop the multilayered films with the good ordering dispersion of SMWCNT and SPES polymers utilizing the layer-by-layer sandwich self-gathering strategy showing a viable and accessible approach to improve the appraisal of PEMs. As expected, the prepared sandwiched nanocomposite of SPES/SMWCNT/SPES owns good stability with low fuel cross over, and high proton conductivity at low cost was investigated.

## 2 | EXPERIMENTAL SECTION

### 2.1 | Materials

Poly(ether sulfone) (PES-Veradel® 3000MP) was purchased commercially from Solvay. Multiwalled carbon nanotube (10-20 nm diameters) procured from Merck. Chlorosulfonic acid (99% purity), sulfuric acid (98% purity), nitric acid (AR, 70%) and *N*,*N*-Dimethylacetamide (DMAc-anhydrous 99.8%) were received from Sigma Aldrich Chemical Pvt. Ltd.

### 2.2 | Functionalization of PES-$SO_3H$ and MWCNT-$SO_3H$

The functionalization of sulfonic acid groups on the PES matrix with the optimized concentration of chlorosulfonic acid and sulfuric acid with 39 ± 0.05% DS was discussed briefly in our previous reported literature.[39] The functionalization of multiwalled carbon nanotubes with sulfonic acid (SMWCNT) was prepared in a two-step synthesis under a nitrogen atmosphere.[40] First, the commercially procured MWCNT (1 g) was purified by adding nitric acid and sulfuric acid in the concentration of 1:1 at 80°C to remove the surface impurity and amorphous carbon. This mixture solution was ultra-sonicated, filtered and washed with deionized water, finally dried in a vacuum giving a total amount of purified MWCNT (p-MWCNT). Second, the sulfonic acid functionalization of MWCNT is made by adding 1 g of p-MWCNT to 100 mL distilled water and ultra-sonicated, followed by heating. The residual dried sample was then added with 40 mL sulfuric acid at 255°C for 20 hours, cooled, washed with deionized water until its pH ~ 7 and dried to produce the SMWCNT.

### 2.3 | Preparation of sandwiched nanocomposite membranes

The dense and compact sandwiched nanocomposite membranes of SPES/SMWCNT/SPES were prepared by depositing the SPES on both sides of SMWCNT as reported from the literature.[41] For the bottom layer preparation, SPES solution (0.5 g of SPES in 5 mL of DMAc) was deposited on the clean petri dish. Alongside the SMWCNT paper (0.5, 1, 1.5 and 2 wt%) was obtained from freeze-drying process based on the reported literature.[41] The SMWCNT paper was mounted onto the top layer of SPES creating the SPES/SMWCNT layer by slightly drying at 80°C for 10 hours. Finally, for the formation of sandwich-type of SPES/SMWCNT/SPES was prepared by casting the solution of SPES on the other side of SMWCNT paper and dried for another 10 hours at 80°C. The pure SPES membrane without the SMWCNT was also synthesized as a contrast membrane via the solvent casting technique. Hereafter, the membranes with 0.5, 1, 1.5 and 2 wt% of SMWCNT within SPES will be labelled as G1, G2, G3 and G4 sandwiched nanocomposite membranes, respectively (Scheme 1).

### 2.4 | Characterization

X-ray diffraction (XRD, X'Pert PRO PANalytical X-ray diffractometer) and Fourier transform infrared spectroscopy (FTIR, Perkin Elmer Spectrophotometer) analyses were carried out to investigate the structural property and functional groups. Raman spectroscopy was studied using Micro-Laser Raman (Seiki, Japan) for the defect study in MWCNT and SMWCNT with an excited wavelength at 633 nm. High-resolution transmission electron microscopy (HR-TEM, JEOL-2100) with an accelerating voltage of 80-200 kV was engaged to analyze the microstructure images of the MWCNT and SMWCNT. Field emission scanning electron microscope (EVO18, CARL ZEISS) and energy dispersive X-ray microanalysis (Quantax 200 with X Flash 6130 instruments) were used to explore the surface morphology, cross-section and quantitative elemental mapping of the samples with the accomplishment of gold sputtering. X-ray photoelectron spectroscopy (XPS, ESCALAB 250xi of Thermo Scientific) was conducted over a scan rate of 0 to 1400 eV with monochromatic X-Ray radiation generated by Al Kα for the SMWCNT. A DSC-TGA analyzer (Universal V4.5A TA Instruments) was used to analysis the membrane weight retention and the thermal stability by thermo gravimetric technique (TGA) in the $N_2$ environment with required flow rate of 45 mL $min^{-1}$. The test was taken in the temperature from 40 to 700°C with a heating rate of

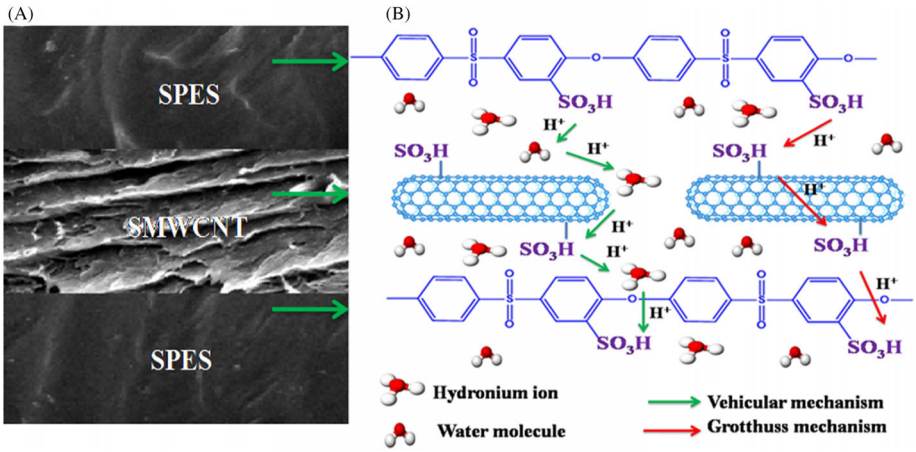


**SCHEME 1** Schematic illustration of A, sandwich structure and B, ionic conduction mechanism

10°C $min^{-1}$. The similar TGA analyzer with the same condition was used to identify the transition temperature of membranes ($T_g$) of the membrane by the DSC technique in the thermal scale of 35 to 200°C. The preheating all the samples above the transition temperature are removes the residual moisture and the solvent in the polymer membranes. Approximately the 0.1 g of membrane sample is necessary for this test. A universal testing machine (UTM, INSTRON 3365) was used to evaluate the mechanical property in terms of the tensile strength (MPa), Young's modulus (MPa) and elongation at break (%).

## 2.5 | Measurements

### 2.5.1 | Oxidative stability

The Fenton test assessed chemical or oxidative stability. The dry-weighted sandwiched nanocomposite membranes were soaked in Fenton's reagent (2 ppm of $FeSO_4$ and 3% of $H_2O_2$) at room temperature, and the degraded percentages of weight in 25 hours were noted.

### 2.5.2 | Water uptake and swelling ratio

The dimensional changes concerning water uptake and swelling ratio of the sandwiched nanocomposite membranes were measured. By the increase/decrease in weight (g) and area ($cm^2$) of the dry samples ($W_{dry}$ and $A_{dry}$) after immersing them in deionized water for 24 hours at predetermined temperatures. Over time, the amount of water absorption was assessed for the wet membranes by weighting again ($W_{wet}$ and $A_{wet}$). The following equation evaluates the water uptake and swelling ratio from the observed values:

$$\text{Change in weight}\,(\%) = \frac{(W\text{wet} - W\text{dry})}{W\text{dry}} \times 100 \quad (1)$$

$$\text{Change in area}\,(\%) = \frac{(A\text{wet} - A\text{dry})}{A\text{dry}} \times 100 \quad (2)$$

### 2.5.3 | Ion exchange capacity and hydration number

A standard acid–base titration measures the ion exchange capacity (IEC) for the sandwiched nanocomposite membranes. In brief, the vacuum dried sandwiched nanocomposite membranes were transferred into the 0.1 M NaCl solution and soaked for 24 hours to exchange $Na^+$ ions in the solution with $H^+$ ions in the membrane. Then the solution was titrated against 0.01 NaOH base solution using phenolphthalein as an indicator, and the IEC (meq $g^{-1}$) was calculated using the following relation:

$$\text{Ion exchange capacity} = \frac{\text{volume} \times \text{normality}}{\text{dry weight of polymer membrane}} \quad (3)$$

where volume and normality are taken for NaOH.

The hydration number ($\lambda$) assists the number of water molecules absorbed per one functional group of sulfonic acid. $\lambda$ was calculated by applying the values in the equation,

$$\lambda = \frac{\text{Water Uptake} \times 10}{\text{IEC} \times \text{Molecular weight of water}} \quad (4)$$

Though $\lambda$ is dimensionless but sometimes expressed as mol $H_2O$/mol $SO_3^-$.

### 2.5.4 | Proton conductivity

The proton conductivity ($\sigma$) for the sandwiched nanocomposite membranes was measured via AC impedance spectroscopy, employing Potentiostat/Galvanostat μ Auto-Lab analyzer. The measurement was done by the two-electrode system with the contact of membrane in the micrometer thickness. The thermo-controlled (30°C-80°C) and relative humidified condition (RH = 100%) was used with the sweeping frequencies over the range of 10 MHz to 10 Hz at an AC signal of 10 mV. The proton conductivity was intended from the resistance value using the equation

$$\sigma = \frac{L}{R \times A} \tag{5}$$

where $\sigma$, $L$, $A$ and $R$ are the proton conductivity (S $cm^{-1}$), membrane thickness (cm), cross-sectional area ($cm^2$) and bulk resistance (Ω), respectively. The calculated activation energy ($E_a$) from the slope of the plot corresponds to proton conductivity against the temperature using the Arrhenius equation

$$Ln(\sigma) = Ln(\sigma_0) - \left(\frac{E_a}{RT}\right) \tag{6}$$

where $\sigma$, $\sigma_0$, $E_a$, $R$ and $T$ are the proton conductivity (S $cm^{-1}$), pre-exponential factor (mS $K^{-1}$ $cm^{-1}$), activation energy (K J $mol^{-1}$), universal gas constant (8.314 J $mol^{-1}$ $K^{-1}$) and absolute temperature (K), respectively.

### 2.5.5 | Single-cell PEMFC performance, durability and $H_2$ permeability test

The membrane electrode assembly (MEA) was fabricated, as reported in our previous studies.[39] The MEA was tested by the Bio-Logic science instrument, with the active cell area of 5 $cm^2$ for the prepared sandwiched nanocomposite membranes. The polarization (I-V) performances of MEA were measured for 100% RH at 80°C with the $H_2$ and $O_2$ feeds at a flow rate of 250 and 500 ccm. After equilibrating the desired levels, the measurement of cell voltage as a function of current and power density was conducted. The durability test of the MEA for the G3 sandwiched nanocomposite membrane was also examined by monitoring open-circuit voltage (OCV) degradation at the same parameter of 80°C in 100% RH for 15 hours. The $H_2$ gas permeability of the membrane specimens was calculated to examine the fuel barrier properties by conventional variable pressure/constant volume method from the literature.[42] Prior to performing the analysis, the membrane was dried at 100°C for 3 h to eliminate the moisture. 1 barrer of pressure rate is maintained during the fed of $H_2$ gas and kept at 30°C during the experiment. The following equation was used to calculate the $H_2$ gas permeability

$$P = DS = \frac{V_{p1}\left(P_{p2} - P_{p1}\right)}{\left[\mathrm{ART}\Delta t\left(P_f - \frac{\left(P_{p2}+P_{p1}\right)}{2}\right)\right]} \tag{7}$$

"$P$" is $H_2$ gas permeability (barrer), "$D$" is diffusivity coefficient ($cm^2$ $S^{-1}$), S is solubility coefficient ($cm^3$ ($cm^2$ scm Hg)$^{-1}$), l is thickness of membrane (cm), $V_p$ is constant permeation volume ($cm^3$), $A$ is area of membranes ($cm^2$), $R$ is the gas constant (J $mol^{-1}$ $K^{-1}$), T the temperature (kelvin), $\Delta t$ is time for pressure change from $P_{p1}$ to $P_{p2}$ and $P_f$ is feed pressure (cm Hg).

## 3 | RESULTS AND DISCUSSION

The XRD patterns of the parental and sulfonated MWCNT are shown in Figure 1A. The two characteristic peaks at 2$\theta$ of 26.6° (002) and 43.4° (100) in MWCNT with a slight difference in peak width of the SMWCNT, signifying the disentanglement and unbundling attained by SMWCNT after the grafting of the sulfonic acid group.[43] Both of the XRD patterns show similar features designating the functionalization of sulfonic acid groups doesn't change or destroys the crystal structure of parental MWCNT.[40] Additionally, the diffraction peaks of SPES and its sandwiched nanocomposite membrane were also shown in Figure 1(b). The pure SPES exhibits amorphous structure, as observed from the broad and halo peak at 2$\theta$ of 18.15°.[44] Further broadened peak in the sandwiched nanocomposite containing various ratios of SMWCNT owns to its less crystalline nature. Actually, in the sandwiched nanocomposite membrane, the OH groups of SPES inhibit the chain packing, and the dense SMWCNT network restricts the crystal growth and making them more amorphous. The peaks of SMWCNT were not identified separately, disclosing the good compatibility of the materials and its interlayer adhesion of sandwiched structure as identified in SEM images. Due to the aggregation effect for 2 wt% of SMWCNT, there is a hike in the intense crystalline peak for the G4 membrane compare to the G3 membrane.

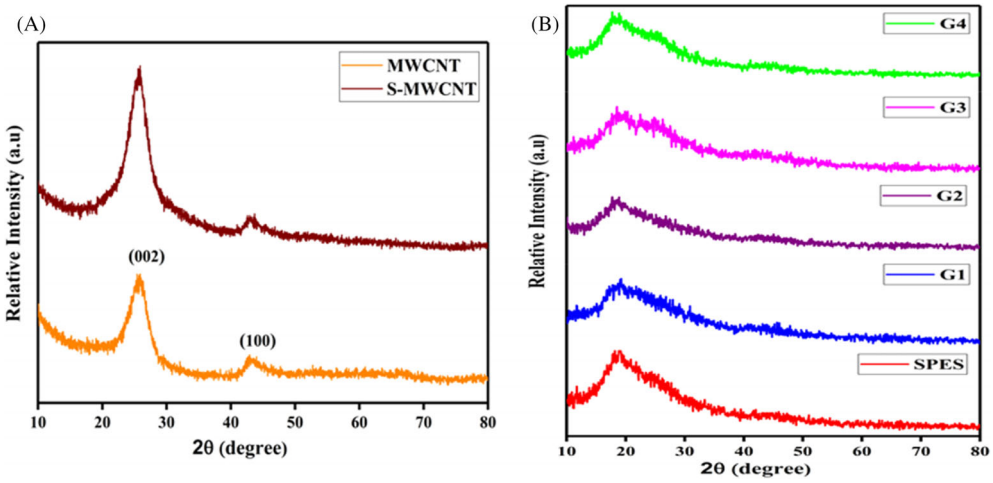


**FIGURE 1** XRD patterns of A, MWCNT and SMWCNT; B, electrolyte membranes of pristine SPES, G1, G2, G3 and G4

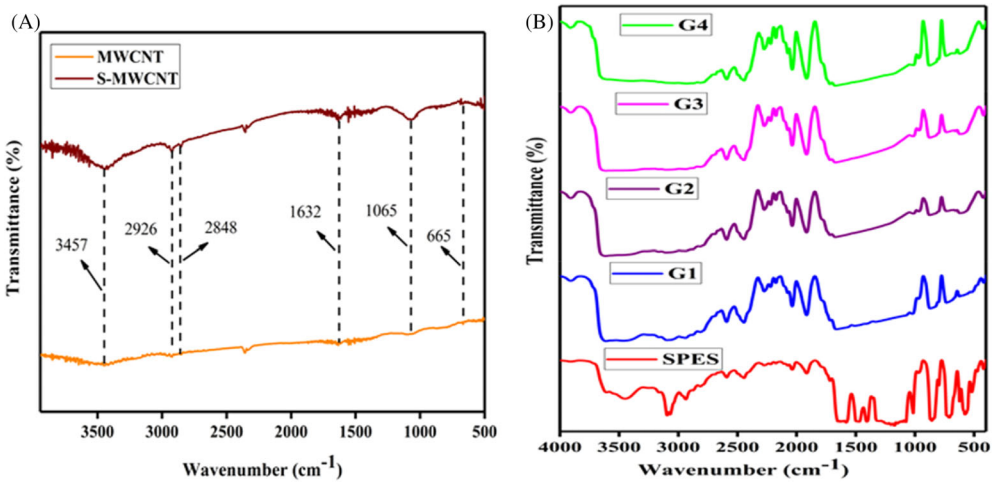


**FIGURE 2** FTIR spectra of A, MWCNT and SMWCNT; B, electrolyte membranes of pristine SPES, G1, G2, G3 and G4

In Figure 2A, the FTIR spectrum of the parental MWCNT with the peak at 1632 $cm^{-1}$ corresponds to the C═C graphitic stretching of mode. And the slightly broad centered peak at 3457 $cm^{-1}$ is attributed to the —OH stretching mode originated by the little moisture containing group. The symmetric and asymmetric stretching vibration band of $CH_2$ is located at 2848 and 2926 $cm^{-1}$, respectively.[45] In SMWCNT, the band present at 1065 and 997 $cm^{-1}$ states the asymmetric and symmetric stretching vibration modes of S—O of the $SO_3$ group.[46] The stretching peak at 665 $cm^{-1}$ confirms the presence of SO stretching mode of —$SO_3H$ group.[47] And the broad band in the region of 3300-3600 $cm^{-1}$ is assigned to the sulfonic group due to the functionalization of sulfonic acid that enhances the OH molecular group. These spectra confirm the successful grafting of the sulfonic acid group on to the walls of MWCNT.[43] The grafting of the PES matrix with sulfonic acid is evident from the result, as the bands at 2930, 2598 and 1636 $cm^{-1}$ symbolize the O—H vibration from sulfonic acid groups, as depicted in Figure 2B. The $SO_3^-$ vibrations from the grafted sulfonic acid group are credited with the bands at 1024, 1287 and 1231 $cm^{-1}$. The successful grafting of sulfonic acid groups on PES is inveterate by the broad peak at 3450 $cm^{-1}$ credits for the hydroxide vibration of the super sulfonic acid group.[25] The SMWCNT integrated between the two single layers of SPES matrix enhances the OH vibration with the presence of sulfonic acid groups on the walls of SMWCNT. This integration shows the better functional group compatibility among the SMWCNT and SPES layer, which was inferred from these FTIR studies.

Raman spectroscopy is analyzed for the parental and sulfonated MWCNT to assess its structural defect, and state of carbon hybridization after the functionalization and illustrated its spectrum in Figure 3. The two bands located around 1330 and 1580 $cm^{-1}$ are present in both samples. At 1330 $cm^{-1}$, the D band is associated with the disorder and defect structure of $sp^2$ hybridization of carbon atoms in nanotubes. The band at 1580 $cm^{-1}$ is set to

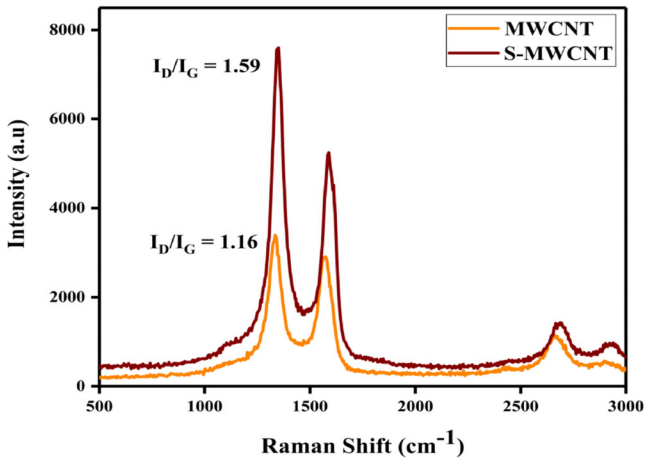


**FIGURE 3** Raman spectra of MWCNT and SMWCNT

G band and related to the graphite tangential vibrational nature (first-order scattering of $E_{2g}$ mode of $sp^2$ hybridized carbon lattice) at the layered mode of the carbon atoms.[46,48] The intensity ratio of two bands for D to G ($I_D/I_G$) of MWCNT and SMWCNT are 1.16 and 1.59, represent the structural deformation and defect. The $I_D/I_G$ ratio for SMWCNT is higher than the parental MWCNT signifying the property of MWCNT at the surface was damaged by introducing sulfonic acid moieties on the $sp^2$ carbon network.[49]

XPS spectra of SMWCNT illustrated the surface elemental composition and chemical valences of the functional groups of sulfonic acids occupied on the surface of MWCNT (S2p) and its inherent groups (C1s and O1s) in Figure 4. The de-convoluted sulfonic acids-treated MWCNT exhibited the five clear spectrums of C1s. The positions of the different peaks are shown at 290.83 eV, 289.53 eV, 288.25, 286.40 and 284.11 eV assigned to C*(O)—O—(O)*C, C*(O)—OH/C—$SO_3H$, C*(O)—OC, C═O and C═C bond, respectively. The O1s spectrum gives four individual contributions related to the peaks of different regions at 533.41, 532.29, 531.85 and 531.16 eV linked to C—OH, C═O, S—OH and S═O bonds, respectively. The two peaks correspond to the spectrum of S2p, associated with the $S2p_{1/2}$ and $S2p_{3/2}$ levels at 169.90 and 168.81 eV, which is connected to sulfonic acids, that confirms the sulfonation on MWCNT.[45] The surface atomic concentration of sulfonic acid functionalized MWCNT was estimated to be 86.19, 12.28 and 1.53 at% for C1s, O1s and S2p elements. Further proof of the confirmation of sulfonation occurred on the surface of MWCNT.[46,47]

In HR-TEM, the structural morphology of parental and sulfonated MWCNT demonstrated the tangled, fiber-like structure, which was preserved still after modification with sulfonic acid groups. The SMWCNT sticks collectively as chains like morphology due to van der Waals mutual interactions among individual tubes. The functionalization of sulfonic acid further separated the single tubes, owed to the ionic repulsion conveying by —$SO_3H$ groups contain in sulfonic acids. The dispersal diameter among individual tubes is higher in SMWCNT, as seen in Figure 5A,B. The individual tubes diameter is smaller in size (10 nm), as shown in Figure 5C. HR-TEM and XRD analysis verify the SMWCNT was modified on sulfonic acids.[46,47] The HR-TEM image in Figure 5C, shows the lattice fringes of SMWCNT and measured the d-spacing values in the orders of 0.333 and 0.334 nm. The corresponding intensity of diffraction peaks was located at 26.6° and 43.4°, analogous to planes (002) and (100). The SAED results from Figure 5D obtained from the HR-TEM were well fitted with XRD values peaks.

The observation of surface morphology for both the parental MWCNT and SMWCNT exhibits the tangled thread-like structure with the diameter ranging 10 to 20 nm represented in Figure 6A. After the sulfonic acid groups functionalization onto the MWCNT, the diameter, morphology and structural distribution do not show any noticeable difference from the parental MWCNT. Also, it lessens the aggregation and resembles the parental features of MWCNT.[41] It is due to the functionalization of sulfonic acid on the walls of MWCNT; there exhibits an electrostatic repulsive force among the individual MWCNT that causes them to separate away and make it a well-dispersed matrix as shown in Figure 6A. The EDS mapping images in Figure 6B show the presence, concentration and evenly distribution of sulfur (S) elemental group along with the carbon (C) and oxygen (O) in SMWCNT in comparison to the presence of C and O elemental groups of MWCNT.[46]

The surface FE-SEM images of the sandwich membrane in Figure 7A clearly expose the smooth and pore free surface of the top layer SPES due to the interconnected polymer micro-structures. The different weight percentage of the SMWCNT in the central layer of sandwich structure doesn't changes the surface of SPES top layer, so it replicated the bare SPES structure with the smooth surface. The cross-sectional FE-SEM of sandwich membranes is displayed in Figure 7B. The plain surface on both the side of the sandwich membrane indicated the thick or dense SPES layers (approximately 35 μm thickness). Specifically, the SMWCNT region in the middle of the sandwich membrane(approximately 40-70 μm thickness) is crumpled and compact structure. These validates the prepared membranes as the sandwiched structure. Owing to the incremental concentrations of SMWCNT, the thickness of the central layers also increases in the sandwich membrane (Table 1). The functionalization of sulfonic acid on the SMWCNT increased the synergy interplay between the SPES layers due to the

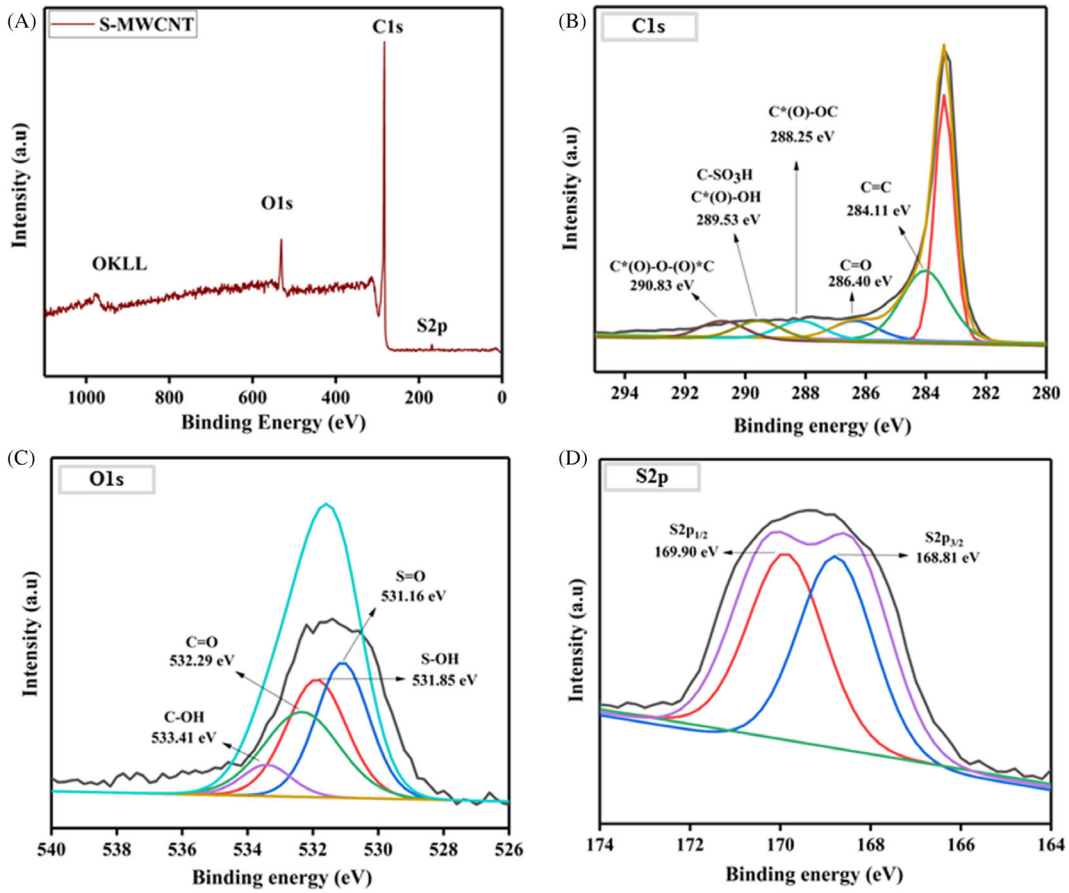


**FIGURE 4** XPS spectra of A, SMWCNT; B, C1s; C, O1s and D, S2p elements

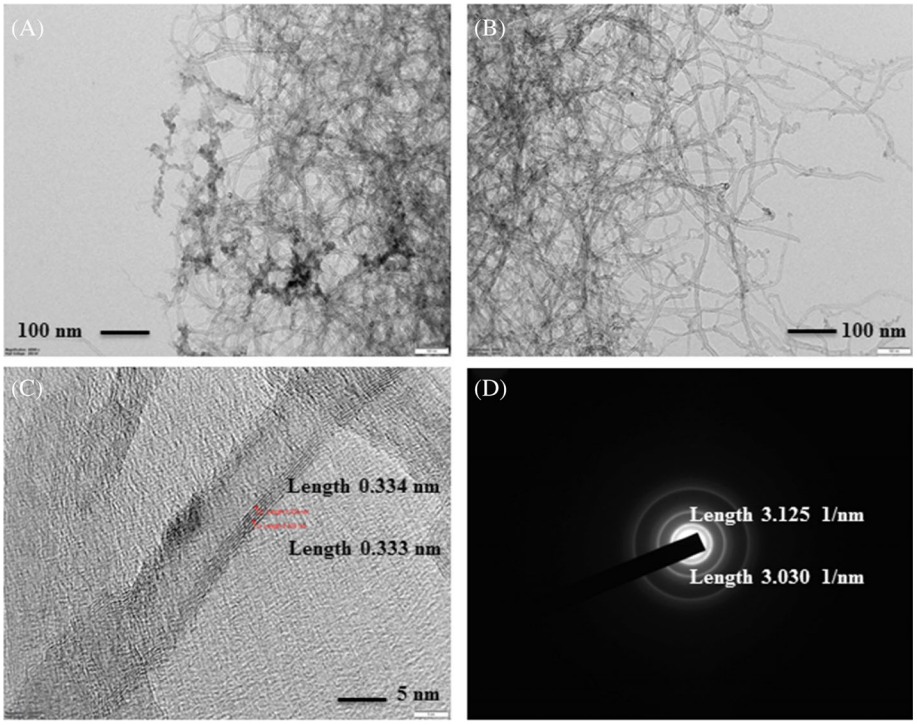


**FIGURE 5** HR-TEM images of A, MWCNT; B, SMWCNT; C, SMWCNT fringes and D, SAED pattern of SMWCNT

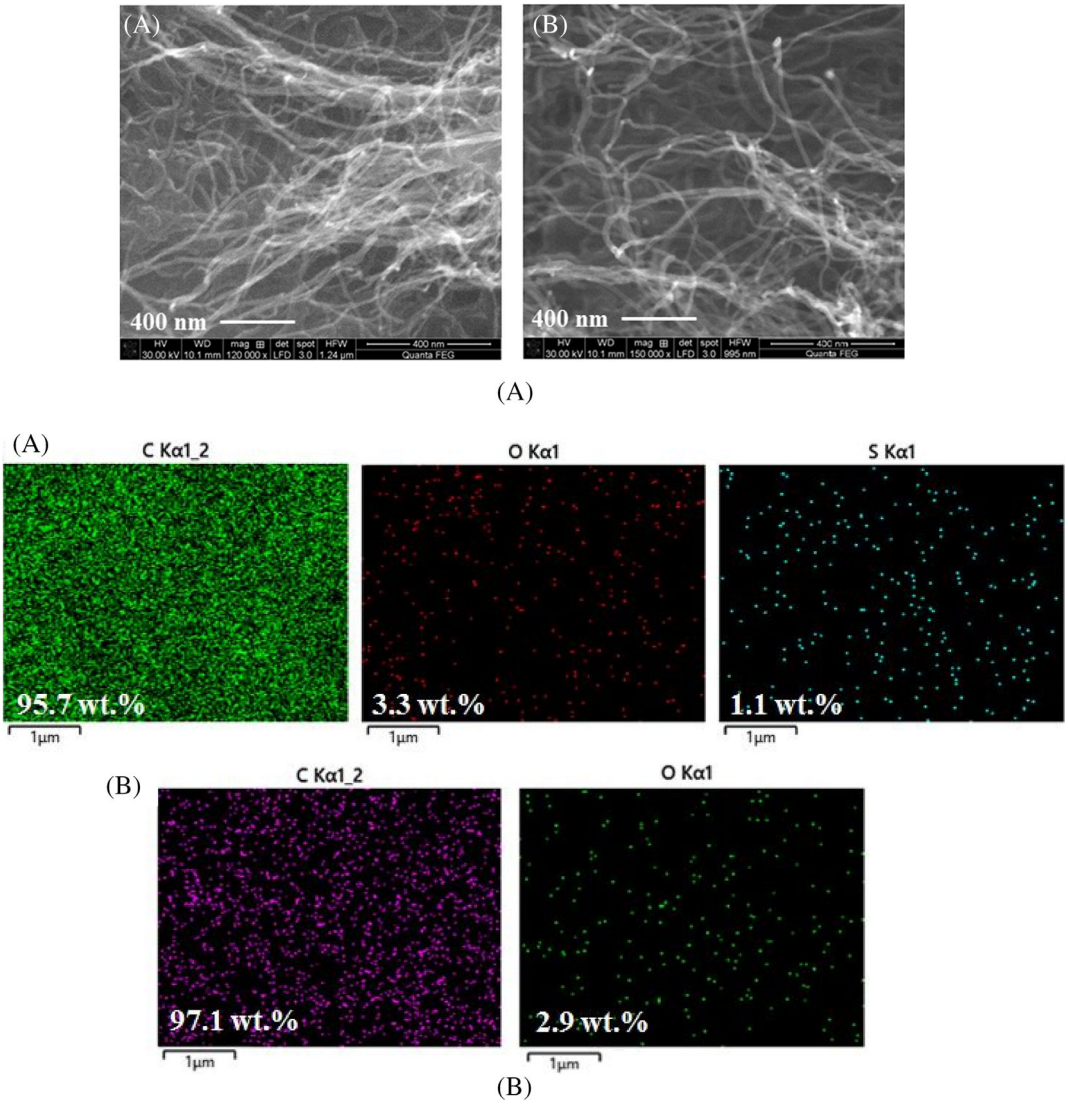


**FIGURE 6** A, FE-SEM images of (A) MWCNT and (B) SMWCNT. B, EDS analysis (insert) and mapping of (A) SMWCNT and (B) MWCNT

more dispersion of the individual tubes in the middle layer, which tend to form the compacted structure with no phase separation or pinholes between SPES/SMWCNT/SPES. As a result, all the sandwich membranes (G1, G2, G3 and G4) are formed with no pores and cracks in the entire morphology. The existence of the higher interface interaction drive the defects free structure between the SPES and SMWCNT, which proves the excellent compatibility of SMWCNT and SPES.[41] The drawback of swelling membranes prepared from the solvent casting technique is well maintained by the dimensional and compactable structure designed from sandwiched type, which is also proven from the swelling ratio analysis.[36]

TGA results of SPES, G1, G2, G3, G4 membranes and SMWCNT were shown in Figure 8A,C. The evaluated data indicates that the SPES sandwich nanocomposite membrane exhibited high thermal stability concerning SPES. For the prepared membranes, the three steps of weight losses are obtained: (a) losses of water molecules in terms of bound and free state at 100 to 150°C, (b) elimination of $SO_3H$ on the aromatic polymer chains of SPES and SMWCNT at 220 to 350°C and (c) dissolution of backbone on SPES chains was initiated above 500°C.[50] The SMWCNT exhibits the residual weight of 87.12% at 700°C. TGA curves of SPES based sandwiched nanocomposites reveal slightly retarded weight loss contrast to SPES likely owed to the electrostatic mutual interactions between the two layers of SPES with the center layer of SMWCNT. The effect of SMWCNT integration between the SPES matrices creates the electrostatic interaction among the two regions due

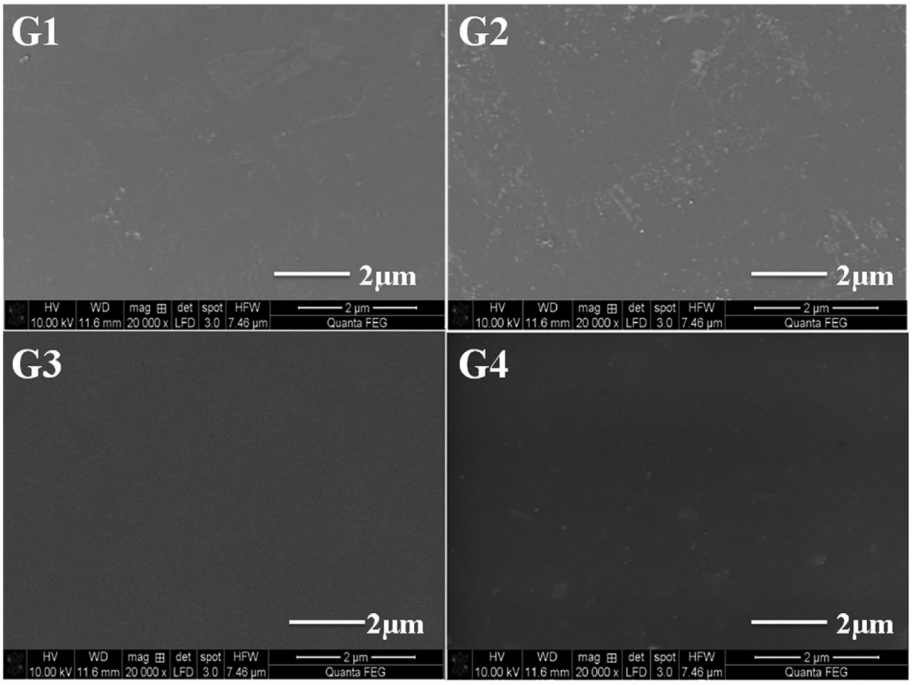


(A)

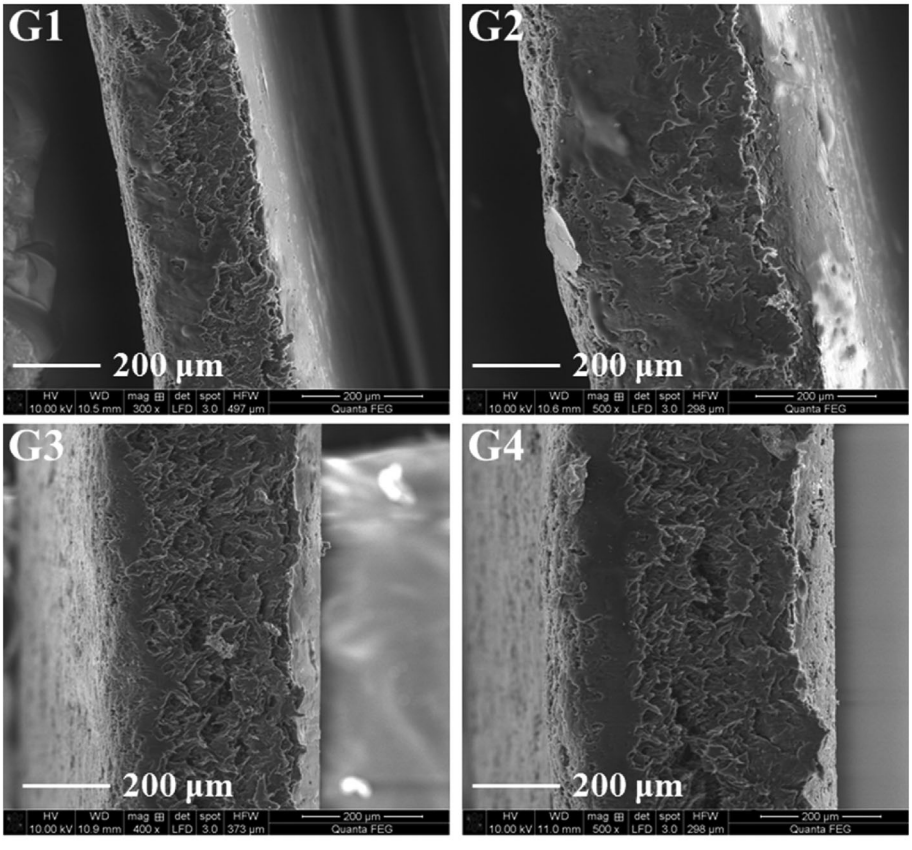


(B)

**FIGURE 7** A, Surface FE-SEM images. B, Cross-sectional FE-SEM images of G1, G2, G3 and G4 electrolyte membranes

to the bearing of sulfonic acids, hydroxyl at the walls of nanotubes, and sulfonic acids on SPES. This interplay constrains the chain movement against the polymer decomposition under the thermal agitation.

Subsequently, the SPES nanocomposite was adequately stable up to 150°C, sufficient to meet the condition for a durable PEM operation. These were further studied by DSC and reliable with TGA data, as revealed

**TABLE 1** Mechanical and oxidative stabilities for the electrolyte membranes of pristine SPES, G1, G2, G3 and G4

| Membranes | Tensile strength (MPa) | Young's Modulus (MPa) | Elongation at break (%) | Oxidative stability (wt%) |
|---|---|---|---|---|
| SPES | 12.3 ± 0.6 | 1248 ± 62 | 29.4 ± 1.4 | 84.2 ± 4.2 |
| G1 | 31.8 ± 1.5 | 1698 ± 84 | 18.9 ± 0.9 | 94.5 ± 4.7 |
| G2 | 35.0 ± 1.7 | 1816 ± 91 | 14.0 ± 0.7 | 95.7 ± 4.7 |
| G3 | 40.0 ± 2.1 | 2208 ± 110 | 11.9 ± 0.5 | 98.1 ± 4.9 |
| G4 | 36.2 ± 1.8 | 1770 ± 88 | 13.4 ± 0.6 | 96.4 ± 4.8 |

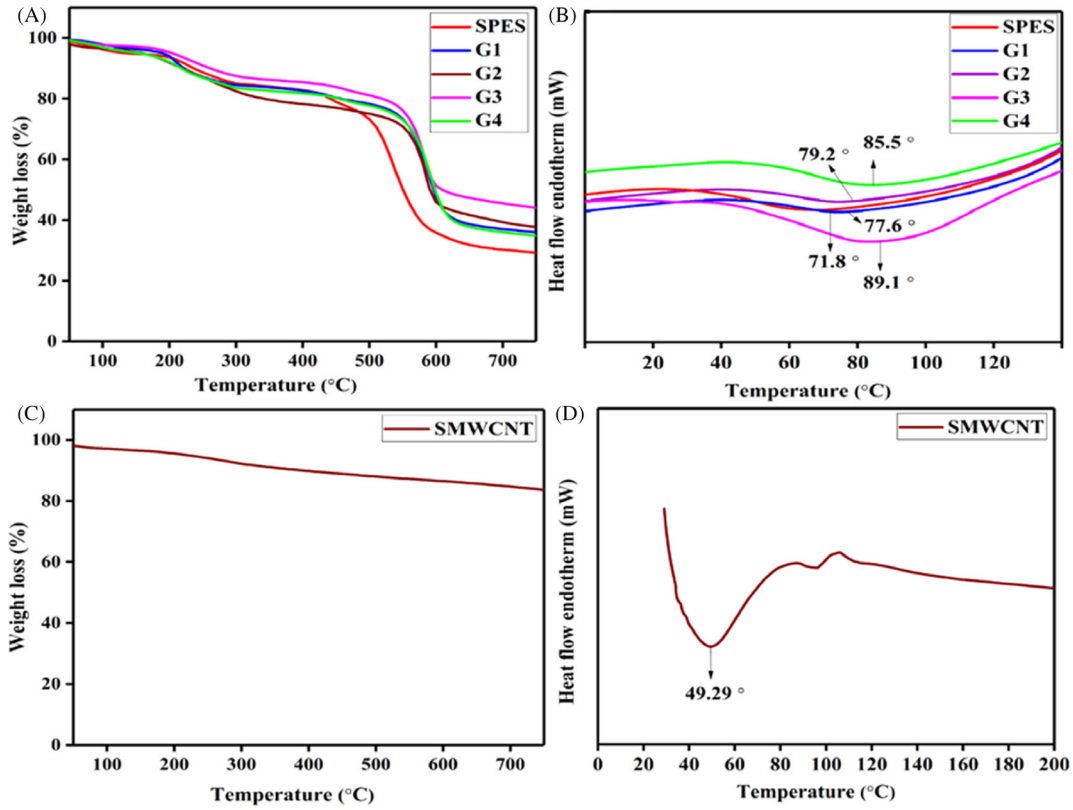


**FIGURE 8** A, TGA; B, DSC curves for the electrolyte membranes; C, TGA and D, DSC curves for SMWCNT

in Figure 8B,D. The effect of grafting of sulfonic acids on MWCNT and sandwich arrangement of SPES with SMWCNT influences glass temperature transition behavior ($T_g$). The structural restructuring of SPES matrices occurred by the sandwich of SMWCNT among the two layers of SPES and created endothermic peaks. The construction of such sandwich type membrane maintained the thermal stability than the pure SPES membrane synthesized from solvent casting technique. This structure conserved both ionic interaction and thermal stability for the fuel cell operating temperature.[34]

As shown in Figure 8B, the endothermic peak at 71.8, 77.6, 79.2, 85.5 and 89.1°C for SPES, G1, G2, G3 and G4 membranes was the glass temperature transition behavior. The SMWCNT exhibits the $T_g$ value at 49.29°C (Figure 8D). The $T_g$ of SPES is around 71.8°C, and further integration of SMWCNT with SPES matrices enhanced the $T_g$ owing to the superior thermal stability of SMWCNT and layered microstructure arrangement. This tendency can be attributed to strong electrostatic ionic interactions between acid-acid pairs at the host interface of SPES in both the upper layer and lower layer of SMWCNT. The SMWCNT was occupied in the mid-layers as more entangled and higher dispersal due to the bearing of sulfonic and causes the more interfacial interplay at SPES interface: SMWCNT. In this mode, the mobility of SPES chains is severely controlled, and therefore extra heat is necessary to get sufficient chain mobility for attaining the phase transition. But certain content of SMWCNT in SPES matrices decreases the $T_g$ due to poor dispersal of SMWCNT by the sequence of higher aggregation effect among them. In general, the DSC results

display the integration of SMWCNT proficiently improves the thermal stability of composite membranes.

The restriction of chain mobility influence the mechanical stability of the membrane is also one of the satisfactory properties for fuel cell performance. The mechanical properties for the prepared sandwiched nanocomposite membrane of SPES are assessed by tensile strength in MPa, elongation at break in %, and Young's modulus in MPa, and depicted as a bar graph in Table 1. The incorporation of SMWCNT enhances the tensile strength and Young's modulus and declines the elongation at break eventually. Also, the sandwiched nanocomposite membrane of SPES reinforced with SMWCNT paves the way for a better compact structure via the interfacial interaction at the interfacial surfaces. The tensile strength and Young's modulus for pure SPES membrane are 12.3 and 1248.8 MPa, while for G3 membrane is 40 and 2208.2 MPa. This incremental mechanical property is due to the strong interconnection of SMWCNT and the SPES matrix through the strong hydrogen bonding and better dispersibility of SMWCNT. Further, the G4 sandwiched nanocomposite membranes mechanical property is reduced owed to the accumulation of poor dispersion of SMWCNT, which disturbs the chain continuity due to the excessive optimized content SMWCNT. The high mechanical stability with a good elongation at break for G3 sandwiched nanocomposite membrane is highly suitable for efficient fuel cell operation.[26,51-53]

During the fuel cell operation, some hydroxyl (HO·) and hydroperoxy (HOO·) radicals might produce at the electrode-electrolyte side. These HO· and HOO· radicals certainly attack the functional groups in the polymer skeleton, which turns out the possible risk of membrane break.[54] Fenton's reagent evaluated the chemical strength of prepared membranes, and its results were displayed in Table 1. The sandwiched nanocomposite membranes can maintain the whole weight more than 24 hours, by contrast to the pure SPES membrane were establish to degradation at 24.5 hours.[55] After 25 hours of the test, the pristine SPES and sandwiched nanocomposite membranes of G1, G2, G3 and G4 retained 84.2, 94.5, 95.7, 98.1 and 96.4% remaining weights. The outcome specifies the introduction of SMWCNT exerted a positive effect on the chemical stability owing to prevent the decomposition of sulfonic acids with radicals. The decomposition of SPES matrices eventually causes in fracture of the membrane. The hydrogen bond cross-linking between the sulfonic acids at the interface of two layers of SPES and SMWCNT matrices aids the productive method for eliminating the degradation of polymer chain's and giving the chemical stability sandwiched nanocomposite membranes. This scheme prevents sulfonic acid dissociation by the best useful interfacial contacts at the SPES and SMWCNT.

The water uptake impacts the mechanical property, dimensional stability and generally the membranes' overall proton conductivity for the efficacious PEM operation. The swelling ratio was also analyzed and which is in common trend as water uptake, and plotted in Figure 9. From these observations, the G3 sandwiched nanocomposite membrane showed the highest water uptake and moderate swelling ratio (66% and 14% at 80°C), represent the strong interfacial interaction among the sandwiched layers than pure SPES (39% and 20% at 80°C). The SMWCNT layer is occupied at the center of two SPES layers bearing the sulfonic acid on the walls of the tubes. Aids the hydrogen bond interaction with the water molecules at two interfacial sites. That facilitates the more occupation of water molecules in between the hydrophilic/hydrophobic channels of SPES matrix. Moreover, the higher dispersivity of SMWCNT in the sandwich-type has a positive effect on water uptake characteristics. It creates a strong hydrogen bonding network between the $SO_3H$ and water molecules in the acid-acid synergistic role that aids the interpenetrating ionic domains and the sandwiched matrices. It connects the more hydrophilic/dead-end channels and creates the mobile transport of proton through the extended range of interconnected channels with continuous pathways.[34]

Meanwhile, the G1, G2 and G4 sandwiched nanocomposite membrane revealed the water uptake and swelling ratio of 46, 59% and 54% and 20, 17% and 16% at 80°C, respectively. When incorporating SMWCNT between the layers of SPES sandwiched assembly, the anisotropic swelling behavior was observed in the in-plane direction. The swelling ratio was considerably diminished by the effectual constraint of SPES polymer

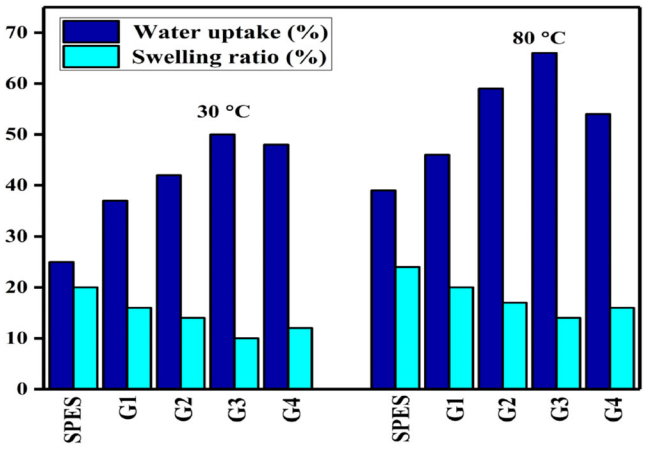


**FIGURE 9** Water uptake and swelling ratio for pure SPES, G1, G2, G3 and G4 membranes at 30°C and 80°C

chain in the swelling direction via the reinforcing effect of SMWCNT on SPES through the good interaction among sulfonic acids at two interfaces. The impact of the high content (2 wt%) of the functional group (SMWCNT) dramatically influences the dimensional property, owning to blocking effect in the SPES membrane matrix. These dominate to reduces the water uptake and puts up swelling ratio, due to the poor acid-acid interaction between the SMWCNT and SPES.[28,55,56]

Interestingly, the IEC estimation is likewise a significant factor, and the IEC value for the pure SPES is 1.51 meq $g^{-1}$. The G1, G2, G3 and G4 revealed the IEC values of 1.69, 1.75, 1.82 and 1.78 meq $g^{-1}$, respectively. Regardless of the inclusion of SMWCNT, the IEC value was increased in G3 sandwiched nanocomposite membrane than the pure SPES. The augmented functional group of $SO_3H$ provided by the SMWCNT in addition to the SPES incremented the transferable proton group in the interpenetrating channels along with the sandwiched matrix at the limited domains.[55] The less dilution and stacking of SMWCNT created a good interfacial interaction with SPES matrix. Subsequently, the formation of proton mediated pathway by the combined effect of enhanced sulfonic acid and interconnecting ionic domains helps better proton conduction within the sandwiched nanocomposite membrane.[26] In contrast, the more stacking and dilution effect has appeared for 2 wt% of SMWCNT, creating the bad interfaces at SPES/SMWCNT/SPES in the sandwiched nanocomposite membrane. The hydration number ($\lambda$) is also linear with water uptake and the IEC parameter. The G3 sandwiched nanocomposite membrane showed the maximum $\lambda$ value of 20.14 associated with more water molecules gathering around the hydrophilic sulfonic acid group.[28]

The proton conductivity measurements were subjected to test at fully humidified condition from 30°C to 80°C for all the prepared membranes and tabulated in Table 2. The pure SPES membrane displayed the proton conductivity value in the range of $11.74 \times 10^{-3}$ S $cm^{-1}$ at 30°C. The SPES polymer matrix contains the sulfonic acids adsorb water-ionic cluster channels and transport protons via vehicular transport. The rise in temperature contributes the lower resistance of the membrane and makes easier the proton diffusion ($20.32 \times 10^{-3}$ S $cm^{-1}$ at 80°C). The intensification in proton conductivity was achieved after the incorporation of SMWCNT (0.5, 1, 1.5 and 2 wt%) into the SPES matrix as a sandwiched type. The sandwich membrane facile the proton transportation using the inter layer adhesion between SMWCNT and SPES layers. It shows the strengthening of proton conductivity of the sandwiched nanocomposite membranes only up to 1.5 wt% of SMWCNT and diminution at 2 wt %. This is due to the dependence of the proton conduction that lies in the structural morphology and interconnection of water cluster channels in the matrix facilitate by the optimized amount of SMWCNT.[10] The 1.5 wt% SMWCNT provides a better interfacial bonding with the water molecules via sulfonic acid groups, which improved the protonic conductive pathway.[52] In particular, the functionalization of sulfonic acid groups on the walls of MWCNT aids the numerous active sites for proton transport and promotes the proton hopping via Vehicular and Grotthuss mechanism. The vehicular mechanism is facilitated by the water molecule channel adsorbed by the sulfonic acid groups of SMWCNT and the Grotthuss mechanism is promoted by the transport of proton from SMWCNT to the SPES polymer or vice versa.[57] The G1, G2, G3 and G4 sandwiched nanocomposite membranes display the proton conductivity and activation energy values of 39.85, 54.45, 72.08, $55.99 \times 10^{-3}$ S $cm^{-1}$ and 10.4, 9.9, 8.8, 9.4 kJ $mol^{-1}$ at 80°C, respectively.

In contrast, the 2 wt% of SMWCNT (G4 membrane) showed less proton conduction than 1.5 wt% SMWCNT (G3 membrane) due to the aggregation and masking of $SO_3H$ groups caused by high cohesive interaction among the SMWCNT.[58] Therefore, low interfacial interaction arises and resulting in impediment of proton transfer for G4 membrane. The superior proton conduction of $72.08 \times 10^{-3}$ S $cm^{-1}$ with low activation energy

**TABLE 2** Thickness, proton conductivity and activation energy for the prepared membranes

| Membranes | Thickness (μm) | Proton conductivity ($10^{-3}$ S $cm^{-1}$) | | | Activation energy |
|---|---|---|---|---|---|
| | | 30°C | 50°C | 80°C | (kJ $mol^{-1}$) |
| SPES | 95±3 | 11.74 ± 0.58 | 14.12 ± 0.70 | 20.32 ± 1.01 | 11.9 ± 0.59 |
| G1 | 115±1 | 30.69 ± 1.53 | 36.43 ± 1.82 | 39.85 ± 1.99 | 10.4 ± 0.52 |
| G2 | 120±5 | 43.15 ± 2.15 | 48.28 ± 2.41 | 54.45 ± 2.72 | 9.9 ± 0.49 |
| G3 | 131±4 | 59.78 ± 2.98 | 64.89 ± 3.24 | 72.08 ± 3.60 | 8.8 ± 0.44 |
| G4 | 143±3 | 48.09 ± 2.40 | 51.91 ± 2.59 | 55.99 ± 2.79 | 9.4 ± 0.47 |

8.8 kJ $mol^{-1}$ was found for the G3 membrane. The SMWCNT with the Nafion membrane also achieved the proton conductivity in the range of 0.03 S $cm^{-1.33}$

The single cell PEMFC performance was evaluated for the sandwiched nanocomposite membranes together with the pure SPES membrane. To overcome the challenges of membrane fabricated via LBL and solvent casting technique, we designed the sandwich structure membranes contains the top and bottom acid SPES polymer layers with central SMWCNT layer that reduces the fuel crossover in the membrane. Figure 10 shows the polarization curve of sandwiched nanocomposite membranes under 100% relative humidity (RH) at 80°C. There is a marginal increase of open-circuit voltage (OCV) from 0.85 to 0.94 V for the pure SPES and G3 membrane, which is 0.09 V higher than the pure SPES. This infers the inclusion of SMWCNT creates a better interaction with SPES polymer and forming a rigid structure along the entire electrolyte matrices that created the higher gas barrier property. The pure SPES membrane attains a peak power output of 75.55 mW $cm^{-2}$ and a current output of 255.71 mA $cm^{-2}$, respectively. The G1, G2, G3 and G4 sandwiched membranes delivered a peak power output of 129.96, 146.91, 173.29 and 157.53 mW $cm^{-2}$ at current output of 511.41, 617.24, 778.26 and 638.28 mA $cm^{-2,}$ which is higher than the SPES membrane. The sandwich membrane comprise the SMWCNT at the central layer that contains the sulfonic acids on the surface of the tubes which aids the uniform dispersion along the matrix and helps to interact strongly with the SPES polymer. This enhanced the synergism mechanism and minimized the ionic and ohmic resistance of the sandwiched nanocomposite membranes.[26,34]

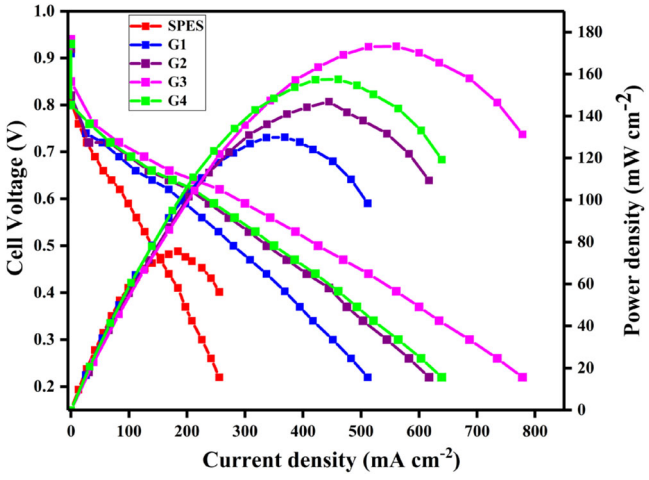


**FIGURE 10** Polarization curve for the electrolyte membranes of pristine SPES, G1, G2, G3 and G4 at 80°C with 100% RH for PEMFC application

Interestingly, the more sulfonic acid groups of SMWCNT can hold extra water molecules and keep the sandwiched nanocomposite membranes adequately wet to encourage water back diffusion. The inclusion of 1.5 wt% SMWCNT within SPES attain higher performance than the 2 wt% due to the even dispersion of SMWCNT promote the better interfacial interplay with the SPES polymer matrix and interconnected the ionic channels. These forbid the fuel crossover that gives a better performance for the G3 membrane. The better compatibility between the electrode, electrolyte, and catalyst region is the crucial part for the better proton transport at the electrode-electrolyte region. The phase boundary at three interfacial layers is enhanced by incorporating the SMWCNT to create the continuous proton-conducting pathway. Simultaneously, encourages the cathode's redox reaction rate and diminished the free radical effect at the electrode-electrolyte region. The combined effect causes enhanced power density with a high gas potential barrier at these interfaces. The G3 membrane achieved a rise in current density (778.26 mA $cm^{-2}$) up to 33% and power density (173.29 mW $cm^{-2}$) up to 43% compared to pure SPES. Overall, this made the remarkable G3 sandwiched nanocomposite membrane the most elevated PEM polarization performer even than the Nafio-115 for the PEMFC.[59] Table 3 shows the SPES sandwich membrane with the other reported literature.

From the polarization performance, the best optimized G3 sandwiched membrane was subjected to a durability test at 100% relative humidity with 80°C for knowing its long-term stability range of OCV as a function of time for 15 hours. The G3 sandwiched nanocomposite membrane revealed an OCV degradation about 0.02 V, as shown in Figure 11A. The inclusion of SMWCNT into the SPES sandwich, creating a strong interlayer interplay, which facilitated the fuel barrier and obstructs the creation of hydroxyl and hydroperoxyl radicals. These effect decelerate the degradation of the membrane and helps the high OCV retention. These shows the positive effect of the functionalized sulfonic acid group on the MWCNT in the sandwiched layers of SPES.[59] It proves that the minimal drop of OCV is due to the higher stability from the sandwich polymer structure and the optimized filler concentration of SMWCNT.

Fuel permeability ($H_2$) in PEM is the vital drawback that reduces the cell performance of fuel cells through diminished fuel efficiency and produced the mixed potential of oxidant and fuel. For superior PEMFC efficiency, the membrane must have a lower amount of fuel permeability and maximum proton selectivity. In the case of the G3 membrane of Figure 11B, the SMWCNT are well dispersed and interacted strongly with the SPES polymer matrix due to the functional groups of sulfonic acids on

**TABLE 3** Summary of PEMs using SPES nano-composite membrane for FC application

| Sample codes from literature | Temperature (°C) | Conductivity (S $cm^{-1}$) | OCV (V) | Current density (mA $cm^{-2}$) | Power density (mW $cm^{-2}$) | References |
|---|---|---|---|---|---|---|
| SPES | 80 | $20.32 \times 10^{-3}$ | 0.85 | 255.71 | 75.55 | This work |
| G3 | 80 | $72.08 \times 10^{-3}$ | 0.94 | 778.26 | 173.29 | This work |
| C3 | 80 | $65.32 \times 10^{-3}$ | 0.90 | 403 | 90 | [3] |
| B3 | 80 | $14.98 \times 10^{-3}$ | 0.92 | 269 | 66 | [4] |
| UiO-66-$NH_2$@NFs-8/ Nafion | 80 | 0.27 | 0.817 | - | 95.49 | [10] |
| MR3 | 90 | $7.9 \times 10^{-2}$ | 0.95 | 354 | 110 | [15] |
| s-$MoS_2$/sPES (5 wt%) | 60 | $14.04 \times 10^{-3}$ | - | 534 | 60 | [20] |
| SPES-MOF | 160 | $41 \times 10^{-3}$ | 0.92 | 889 | 238 | [24] |
| SPES/PWA-30 | 90 | $116 \times 10^{-3}$ | 0.6 | 196 | 307 | [26] |
| SPES/BCNO | 80 | $42.2 \times 10^{-3}$ | 0.93 | 397 | 117 | [39] |
| SPES/SPVdF-HFP-20 | 90 | $78 \times 10^{-3}$ | 0.95 | 633.18 | 262.78 | [60] |
| SPAE/GO/PWA (36 wt%) | 70 | 186.3 at 90°C | 0.95 | 276 | 193.3 | [61] |
| SPAES-LA-X12Y28 | 60 | 158.4 at 90°C | 0.95 | 374 | 232.02 | [62] |
| Nafion-115 | 60 | - | - | 174 | 114.6 | [59] |

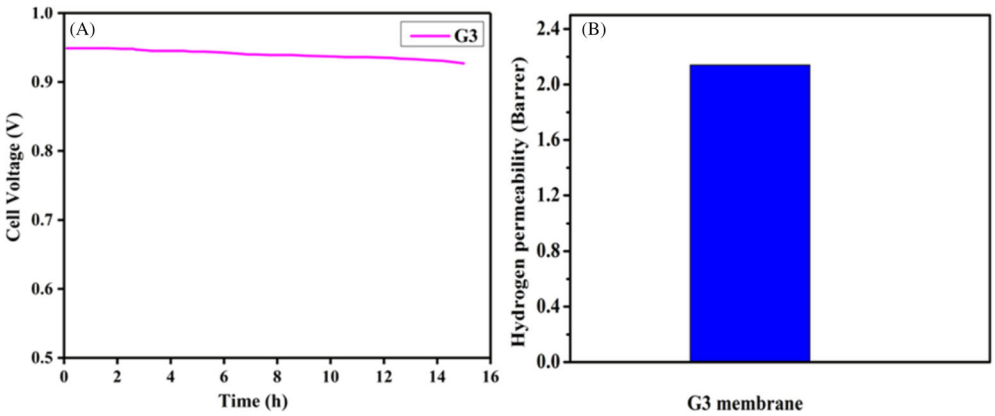


**FIGURE 11** A, Accelerated durability test operation at 80°C under 100% RH for 15 hours and B, $H_2$ permeability of G3 membrane

the SMWCNT retarded the mutual attractions between them and produce the good compatibility effect with the host polymer. This driven the good interfacial adhesion along the SPES sandwich membrane and in turn, causes the barrier networks for $H_2$ gas crossover (2.14 barrer).[42]

## 4 | CONCLUSIONS

Novel sandwich nanocomposite membranes of SPES/SMWCNT/SPES were fabricated by the assembly of SMWCNT layer between the SPES layers. The SPES/SMWCNT/SPES membranes exhibited the flexible and superior interlayer adhesion to create the compact structure which enhance the thermal-mechanical, physico-chemical and electrochemical properties than bare SPES. The interaction of $SO_3H$ groups between SPES and SMWCNT forms a continuous proton-conducting networks via hydrogen bonding, which strengthens the proton conductivity. As the results, the sandwich nanocomposite membranes with 1.5 wt% of SMWCNT (G3) exhibited improved electrochemical performance compared to other PEMs. The durability and $H_2$ permeability test confirms the effective design of the high performance PEM.

## ACKNOWLEDGEMENTS

Authors acknowledge the scheme MHRD-RUSA PHASE-2.0, New Delhi, for financial support. And also thank the UGC-SAP DRS-III, DST-FIST and DST-PURSE for extending the characterization facility in Alagappa University.

## CONFLICT OF INTEREST

There are no conflicts to declare.

## ORCID

*Gayathri Ravi Kumar* https://orcid.org/0000-0003-0323-784X
*Cao Guozhong* https://orcid.org/0000-0001-6539-0490
*Ramesh Prabhu Manimuthu* https://orcid.org/0000-0002-6492-868X


## REFERENCES


1. Ahmadian-Alam L, Mahdavi H. A novel polysulfone-based ternary nanocomposite membrane consisting of metal-organic framework and silica nanoparticles: as proton exchange membrane for polymer electrolyte fuel cells. *Renew Energy*. 2018;126:630-639. https://doi.org/10.1016/j.renene.2018.03.075
2. Liu J, Yu L, Cai X, et al. Sandwiching h-BN monolayer films between sulfonated poly(ether ether ketone) and nafion for proton exchange membranes with improved ion selectivity. *ACS Nano*. 2019;13:2094-2102. https://doi.org/10.1021/acsnano.8b08680
3. Mariappan RP, Cao G, Manimuth RP. Cross-linked SPEEK−PEG−APTEOS-modified $CaTiO_3$ perovskites for efficient acid−base cation-exchange membrane fuel cell. *Energy Fuel*. 2020;34:10087-10099. https://doi.org/10.1021/acs.energyfuels.0c01933
4. Raja K, Pugalenthi MR, Prabhu MR. Investigation on the sulfonatedpoly(ether etherketone)/poly(amide-imide)/barium cerate-based nanocomposite membrane for proton exchange membrane fuel cells. *Int J Energy Res*. 2021;45:8564-8576. https://doi.org/10.1002/er.6393
5. Yan XH, Wu R, Xu JB, Luo Z, Zhao TS. A monolayer graphene—Nafion sandwich membrane for direct methanol fuel cells. *J Power Sources*. 2016;311:188-194. https://doi.org/10.1016/j.jpowsour.2016.02.030
6. Zhang H, Shen PK. Recent development of polymer electrolyte membranes for fuel cells. *Chem Rev*. 2012;112:2780-2832. https://doi.org/10.1021/cr200035s
7. Wang Y, Ruiz Diaz DF, Chen KS, Wang Z, Adroher XC. Materials, technological status, and fundamentals of PEM fuel cells—a review. *Mater Today*. 2020;32:178-203. https://doi.org/10.1016/j.mattod.2019.06.005
8. Shaari N, Kamarudin SK. Recent advances in additive-enhanced polymer electrolyte membrane properties in fuel cell applications: an overview. *Int J Energy Res*. 2019;43:2756-2794. https://doi.org/10.1002/er.4348
9. Shaari N, Kamarudin SK, Bahru R. Carbon and graphene quantum dots in fuel cell application: an overview. *Int J Energy Res*. 2021;45:1396-1424. https://doi.org/10.1002/er.5889
10. Wang L, Deng N, Liang Y, Ju J, Cheng B, Kang W. Metal-organic framework anchored sulfonated poly(ether sulfone) nanofibers as highly conductive channels for hybrid proton exchange membranes. *J Power Sources*. 2020;450:227592. https://doi.org/10.1016/j.jpowsour.2019.227592
11. Oroujzadeh M, Mehdipour-Ataei S, Esfandeh M. Microphase separated sepiolite-based nanocomposite blends of fully sulfonated poly(ether ketone)/non-sulfonated poly(ether sulfone) as proton exchange membranes from dual electrospun mats. *RSC Adv*. 2015;5:72075-72083. https://doi.org/10.1039/c5ra12335f
12. Mariappan RP, Liu C, Cao G, Manimuthu RP. Tailoring SPEEK/SPVdF-co-HFP/$La_2Zr_2O_7$ ternary composite membrane for cation exchange membrane fuel cells. *Ind Eng Chem Res*. 2020;59:4881-4894. https://doi.org/10.1021/acs.iecr.9b06922
13. Munavalli BB, Karidurаganavar MY. Development of novel sulfonic acid functionalized zeolites incorporated composite proton exchange membranes for fuel cell application. *Electrochim Acta*. 2019;296:294-307. https://doi.org/10.1016/j.electacta.2018.11.056
14. Chen RM, Xu FZ, Fu K, et al. Enhanced proton conductivity and dimensional stability of proton exchange membrane based on sulfonated poly(arylene ether sulfone) and graphene oxide. *Mater Res Bull*. 2018;103:142-149. https://doi.org/10.1016/j.materresbull.2018.02.036
15. Martina P, Gayathri R, Pugalenthi MR, Cao G, Liu C, Prabhu MR. Nano-sulfonated silica incorporated SPEEK/S-PVdF-HFP polymer blend membrane for PEM fuel cell application. *Ionics*. 2020;26:3447-3458. https://doi.org/10.1007/s11581-020-03478-9
16. Pugalenthi MR, Prabhu MR. The Pore filled SPEEK nanofibers matrix combined with ethylene diamine modified $SrFeO_3$ nanoneedles for the cation exchange membrane fuel cells. *J Taiwan Inst Chem Eng*. 2021;122:136-147. https://doi.org/10.1016/j.jtice.2021.04.054
17. Mohammadi M, Ataei SM. Structural investigation on bulky aliphatic-aromatic poly(aryl sulfone)s for fuel cell performance. *React Funct Polym*. 2020;155:104692. https://doi.org/10.1016/j.reactfunctpolym.2020.104692
18. Haragirimana A, Ingabire PB, Zhu Y, et al. Four-polymer blend proton exchange membranes derived from sulfonated poly(aryl ether sulfone)s with various sulfonation degrees for application in fuel cells. *J Membr Sci*. 2019;583:209-219. https://doi.org/10.1016/j.memsci.2019.04.014
19. Zhang Q, Zhang Q, Zhang S, Li S. Synthesis and characterization of sulfonated poly(aryl ether sulfone) containing pendent quaternary ammonium groups for proton exchange membranes. *J Membr Sci*. 2010;354:23-31. https://doi.org/10.1016/j.memsci.2010.02.068
20. Yadav V, Niluroutu N, Bhat SD, Kulshrestha V. Sulfonated molybdenum sulfide based sulfonated poly(ether sulfone) composite membranes: ionic transport properties and direct methanol fuel cell performance. *Mater Adv*. 2020;1:820-829. https://doi.org/10.1039/D0MA00197J
21. Gahlot S, Kulshrestha V. White graphene based composite proton exchange membrane: improved durability and proton conductivity. *Int J Hydrogen Energy*. 2018;43:21683-21689. https://doi.org/10.1016/j.ijhydene.2018.05.051
22. Bagheri A, Salarizadeh P, Hazer MSA, Hosseinabadi P, Kashefi S, Beydaghi H. The effect of adding sulfonated $SiO_2$ nanoparticles and polymer blending on properties and performance of sulfonated poly ether sulfone membrane: fabrication and optimization. *Electrochim Acta*. 2019;295:875-890. https://doi.org/10.1016/j.electacta.2018.10.197
23. Alenazi NA, Hussein MA, Alamry KA, Asiri AM. Modified polyether-sulfone membrane: a mini review. *Des Monomers Polym*. 2017;20:532-546. https://doi.org/10.1080/15685551.2017.1398208
24. Anahidzade N, Abdolmaleki A, Dinari M, Firouz Tadavani K, Zhiani M. Metal-organic framework anchored sulfonated

poly(ether sulfone) as a high temperature proton exchange membrane for fuel cells. *J Membr Sci*. 2018;565:281-292. https://doi.org/10.1016/j.memsci.2018.08.037
25. Gahlot S, Sharma PP, Kulshrestha V, Jha PK. SGO/SPES-based highly conducting polymer electrolyte membranes for fuel cell application. *ACS Appl Mater Interfaces*. 2014;6:5595-5601. https://doi.org/10.1021/am5000504
26. Kim AR, Park CJ, Vinothkannan M, Yoo DJ. Sulfonated poly ether sulfone/heteropoly acid composite membranes as electrolytes for the improved power generation of proton exchange membrane fuel cells. *Compos Part B Eng*. 2018;155:272-281. https://doi.org/10.1016/j.compositesb.2018.08.016
27. Xu X, Li R, Tang C, et al. Cellulose nanofiber-embedded sulfonated poly (ether sulfone) membranes for proton exchange membrane fuel cells. *Carbohydr Polym*. 2018;184:299-306. https://doi.org/10.1016/j.carbpol.2017.12.074
28. Divya K, Rana D, Saraswathi MSSA, Bhat SD, Shukla A, Nagendran A. Investigation of the versatility of SPES membranes customized with sulfonated molybdenum disulfide nanosheets for DMFC applications. *Int J Hydrogen Energy*. 2020;45:15507-15520. https://doi.org/10.1016/j.ijhydene.2020.04.019
29. Zhang C, Zhuang X, Li X, et al. Chitin nanowhisker-supported sulfonated poly(ether sulfone) proton exchange for fuel cell applications. *Carbohydr Polym*. 2016;140:195-201. https://doi.org/10.1016/j.carbpol.2015.12.029
30. Zhang Y, Wang H, Yu W, Shi J, Shi H. Sulfonated poly(ether ether ketone)-based hybrid membranes containing polydopamine-decorated multiwalled carbon nanotubes with acid-base pairs for all vanadium redox flow battery. *J Membr Sci*. 2018;564:916-925. https://doi.org/10.1016/j.memsci.2018.07.065
31. Lehman JH, Terrones M, Mansfield E, Hurst KE, Meunier V. Evaluating the characteristics of multiwall carbon nanotubes. *Carbon*. 2011;49:2581-2602. https://doi.org/10.1016/j.carbon.2011.03.028
32. George N, Bipinbal PK, Bhadran B, Mathiazhagan A, Joseph R. Segregated network formation of multiwalled carbon nanotubes in natural rubber through surfactant assisted latex compounding: a novel technique for multifunctional properties. *Polymer*. 2017;112:264-277. https://doi.org/10.1016/j.polymer.2017.01.082
33. Yin C, Li J, Zhou Y, Zhang H, Fang P, He C. Enhancement in proton conductivity and thermal stability in Nafion enhancement in proton conductivity and thermal stability in Nafion membranes induced by incorporation of sulfonated carbon nanotubes. *ACS Appl Mater Interfaces*. 2018;10:14026-14035. https://doi.org/10.1021/acsami.8b01513
34. Bakangura E, Ge L, Muhammad M, Pan J, Wu L, Xu T. Sandwich structure SPPO/BPPO proton exchange membranes for fuel cells: morphology–electrochemical properties relationship. *J Membr Sci*. 2015;475:30-38. https://doi.org/10.1016/j.memsci.2014.09.039
35. Kannan A, Aili D, Cleemann LN, Li Q, Jensen JO. Three-layered electrolyte membranes with acid reservoir for prolonged lifetime of high-temperature polymer electrolyte membrane fuel cells. *Int J Hydrogen Energy*. 2020;45:1008-1017. https://doi.org/10.1016/j.ijhydene.2019.10.186
36. Jia T, Shen S, Xiao L, Jin J, Zhao J, Che Q. Constructing multi-layered membranes with layer-by-layer self-assembly technique based on graphene oxide for anhydrous proton exchange membranes. *Eur Polym J*. 2020;122:109362. https://doi.org/10.1016/j.eurpolymj.2019.109362
37. Che Q, Fan H, Duan X, Feng F, Mao W, Han X. Layer by layer self-assembly fabrication of high temperature proton exchange membrane based on ionic liquids and polymers. *J Mol Liq*. 2018;269:666-674. https://doi.org/10.1016/j.molliq.2018.08.030
38. Li C, Huang N, Jiang Z, et al. Sulfonated holey graphene oxide paper with SPEEK membranes on its both sides: a sandwiched membrane with high performance for semi-passive direct methanol fuel cells. *Electrochim Acta*. 2017;250:68-76. https://doi.org/10.1016/j.electacta.2017.08.058
39. Gayathri R, Prabhu MR. Protonated state and synergistic role of $Nd^{3+}$doped barium cerate perovskite for the enhancement of ionic pathways in novel sulfonated polyethersulfone for $H_2/O_2$ fuel cells. *Soft Matter*. 2020;16:4220-4233. https://doi.org/10.1039/d0sm00427h
40. Naeimi H, Dadaei M. Functionalized multi-walled carbon nanotubes as an efficient reusable heterogeneous catalyst for green synthesis of N-substituted pyrroles in water. *RSC Adv*. 2015;5:76221-76228. https://doi.org/10.1039/C5RA12185J
41. Li C, Xiao L, Jiang Z, et al. Sulfonic acid functionalized graphene oxide paper sandwiched in sulfonated poly(ether ether ketone): a proton exchange membrane with high performance for semi-passive direct methanol fuel cells. *Int J Hydrogen Energy*. 2017;42:16731-16740. https://doi.org/10.1016/j.ijhydene.2017.05.126
42. Vinothkannan M, Kim AR, Nahm KS, Yoo DJ. Ternary hybrid (SPEEK/SPVdF-HFP/GO) based membrane electrolyte for the applications of fuel cells: profile of improved mechanical strength, thermal stability and proton conductivity. *RSC Adv*. 2016;6:108851-108863. https://doi.org/10.1039/C6RA22295A
43. Xu H, Xie Y, Zhu E, et al. Supertough and ultrasensitive flexible electronic skin based on nanocellulose / sulfonated carbon nanotube hydrogel films. *J Mater Chem A*. 2020;8:6311-6318. https://doi.org/10.1039/D0TA00158A
44. Elakkiya S, Arthanareeswaran G, Venkatesh K, Kweon J. Enhancement of fuel cell properties in polyethersulfone and sulfonated poly (ether ether ketone) membranes using metal oxide nanoparticles for proton exchange membrane fuel cell. *Int J Hydrogen Energy*. 2018;43:21750-21759. https://doi.org/10.1016/j.ijhydene.2018.04.094
45. Wei Y, Ling X, Zou L, Lai D, Lu H, Xu Y. A facile approach toward preparation of sulfonated multi-walled carbon nanotubes and their dispersibility in various solvents. *Colloids Surf A Physicochem Eng Asp*. 2015;482:507-513. https://doi.org/10.1016/j.colsurfa.2015.07.005
46. Ge Y, Li Z, Xiao D, Xiong P, Ye N. Sulfonated multi-walled carbon nanotubes for the removal of copper (II) from aqueous solutions. *J Ind Eng Chem*. 2014;20:1765-1771. https://doi.org/10.1016/j.jiec.2013.08.030
47. Guan Q, Li Y, Chen Y, et al. Sulfonated multi-walled carbon nanotubes for biodiesel production through triglycerides transesterification. *RSC Adv*. 2017;7:7250-7258. https://doi.org/10.1039/c6ra28067f
48. Ste NJ, Parthiban V, Sahu AK. Uncovering Nafion-multiwalled carbon nanotube hybrid membrane for prospective polymer

electrolyte membrane fuel cell under low humidity. *J Membr Sci*. 2018;563:65-74. https://doi.org/10.1016/j.memsci.2018.05.051

49. Devaraju S, Lee T, Mohanty AK, et al. Fabrication of durable and flexible single-walled carbon nanotube transparent conductive films. *RSC Adv*. 2017;7:19267-19272. https://doi.org/10.1039/c7ra01180f
50. Díez-Pascual AM, Martínez G, González-Domínguez JM, Ansón A, Martínez MT, Gómez MA. Grafting of a hydroxylated poly(ether ether ketone) to the surface of single-walled carbon nanotubes. *J Mater Chem*. 2010;20:8285-8296. https://doi.org/10.1039/c0jm01238f
51. Shukla A, Bhat SD, Pillai VK. Simultaneous unzipping and sulfonation of multi-walled carbon nanotubes to sulfonated graphene nanoribbons for nanocomposite membranes in polymer electrolyte fuel cells. *J Membr Sci*. 2016;520:657-670. https://doi.org/10.1016/j.memsci.2016.08.019
52. Cai Z, Li R, Xu X, et al. Embedding phosphoric acid-doped cellulose nanofibers into sulfonated poly (ether sulfone) for proton exchange membrane. *Polymer*. 2018;156:179-185. https://doi.org/10.1016/j.polymer.2018.10.013
53. Muthumeenal A, Pethaiah SS, Nagendran A. Investigation of SPES as PEM for hydrogen production through electrochemical reforming of aqueous methanol. *Renew Energy*. 2016;91:75-82. https://doi.org/10.1016/j.renene.2016.01.042
54. Cai Y, Yue Z, Teng X, Xu S. Radiation grafting graphene oxide reinforced polybenzimidazole membrane with a sandwich structure for high temperature proton exchange membrane fuel cells in anhydrous atmosphere. *Eur Polym J*. 2018;103:207-213. https://doi.org/10.1016/j.eurpolymj.2018.02.020
55. Elakkiya S, Arthanareeswaran G, Ismail AF, Das DB, Suganya R. Polyaniline coated sulfonated $TiO_2$ nanoparticles for effective application in proton conductive polymer membrane fuel cell. *Eur Polym J*. 2019;112:696-703. https://doi.org/10.1016/j.eurpolymj.2018.10.036
56. Wang H, Wang X, Fan T, et al. Fabrication of electrospun sulfonated poly(ether sulfone) nanofibers with amino modified $SiO_2$ nanosphere for optimization of nanochannels in proton exchange membrane. *Solid State Ion*. 2020;349:115300. https://doi.org/10.1016/j.ssi.2020.115300
57. Yun S, Im H, Heo Y, Kim J. Crosslinked sulfonated poly(vinyl alcohol)/sulfonated multi-walled carbon nanotubes nanocomposite membranes for direct methanol fuel cells. *J Membr Sci*. 2011;380:208-215. https://doi.org/10.1016/j.memsci.2011.07.010
58. Basri H, Irfan M, Irfan M, Lau WJ, Kartohardjono S. Quantitative analysis of MWCNT agglomeration in polymeric-based membranes using atomic force microscope. *Surf Interface Anal*. 2017;49:55-62. https://doi.org/10.1002/sia.6057
59. Rhan A, Vinothkannan M, Ho M, Lee J, Lee H. Amine functionalized carbon nanotube (ACNT) filled in sulfonated poly ( ether ether ketone ) membrane: effects of ACNT in improving polymer electrolyte fuel cell performance under reduced relative humidity. *Compos Part B*. 2020;188:107890. https://doi.org/10.1016/j.compositesb.2020.107890
60. Kim AR, Vinothkannan M, Yoo DJ. Fabrication of binary sulfonated poly ether sulfone and sulfonated polyvinylidene fluoride-co-hexafluoro propylene blend membrane as efficient electrolyte for proton exchange membrane fuel cells. *Bull Korean Chem Soc*. 2018;39:913-919. https://doi.org/10.1002/bkcs.11489
61. Ryu SK, Kim AR, Vinothkannan M, Lee KH, Chu JY, Yoo DJ. Enhancing physicochemical properties and single cell performance of sulfonated poly(arylene ether) (SPAE) membrane by incorporation of phosphotungstic acid and graphene oxide: a potential electrolyte for proton exchange membrane fuel cells. *Polymers*. 2021;13:2364. https://doi.org/10.3390/polym13142364
62. Lee KH, Chu JY, Mohanraj V, Kim AR, Song MH, Yoo DJ. Enhanced ion conductivity of sulfonated poly(arylene ether sulfone) block copolymers linked by aliphatic chains constructing wide-range ion cluster for proton conducting electrolytes. *Int J Hydrogen Energy*. 2020;45:29297-29307. https://doi.org/10.1016/j.ijhydene.2020.07.197

**How to cite this article:** Ravi Kumar G, Guozhong C, Manimuthu RP. Sandwich assembly of sulfonated poly (ether sulfone) with sulfonated multiwalled carbon nanotubes as an efficient architecture for enhanced electrolyte performance in $H_2/O_2$ fuel cells. *Int J Energy Res*. 2022;46(3):2567-2584. doi:10.1002/er.7329